

Injectable liposome-containing click hydrogel microparticles for release of macromolecular cargos

Luisa L Palmese^a, Paige J. LeValley^c, Lina Pradhan^c, Amanda L. Parsons^d, John S. Oakey^d, Mathew Abraham^e, Suzanne M. D'Addio^f, April M. Kloxin^{a,c*}, Yingkai Liang^{f*}, and Kristi L. Kiick^{a,b*}

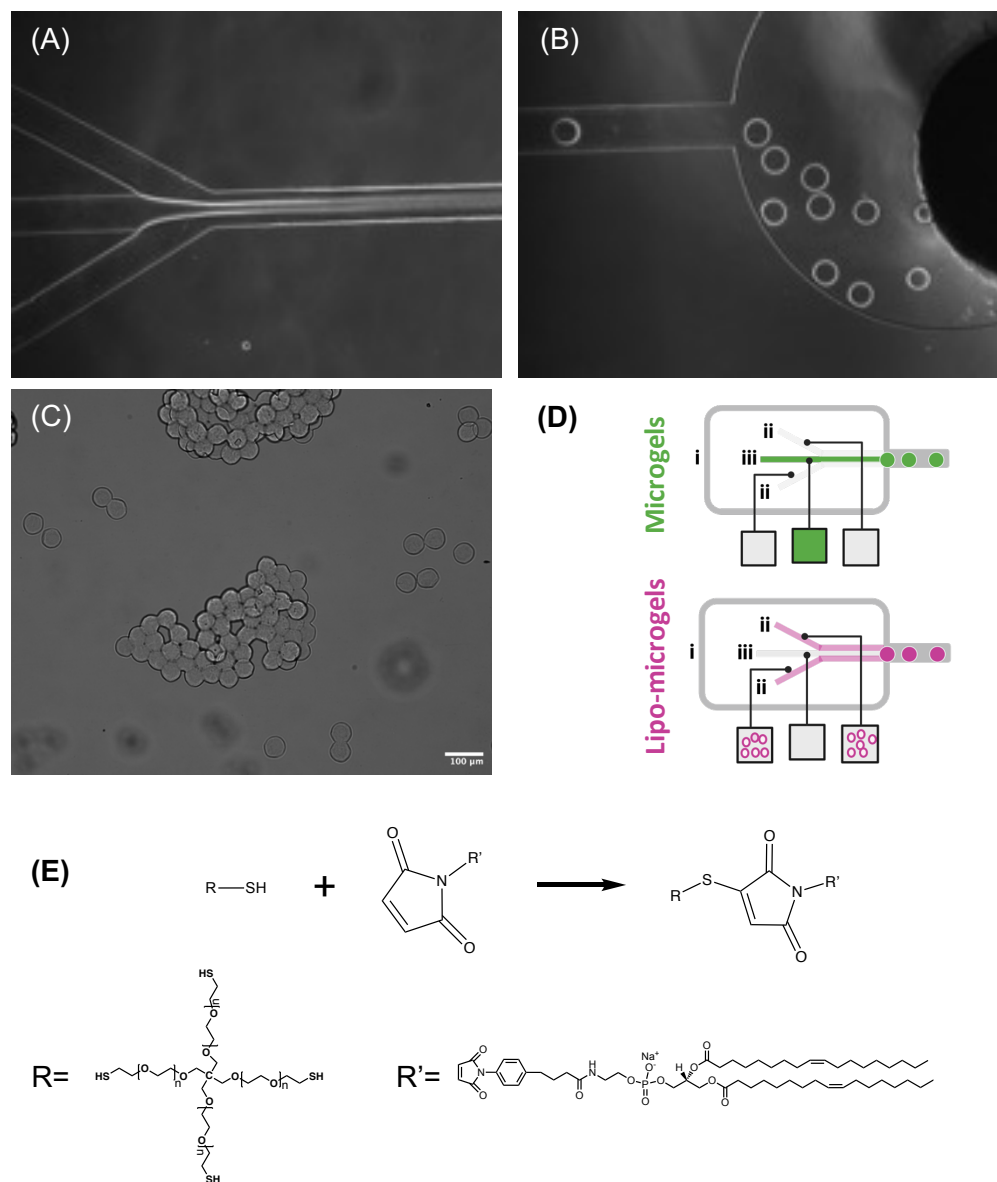


Figure S1: Microfluidic channel after start-up and equilibration (A) as well as outlet channel showing the formation of spherical microgels (B). Representative image of aggregated microgels (C). (D) Design of microfluidic chip for formation of PEG microgels; i. oil stream; ii. PEG-SH₄ and PEG-VS₄ streams; iii. buffer stream for microgels (green) and lipo-microgels (pink). (E) Reaction scheme of MI-lipid to PEG-SH.

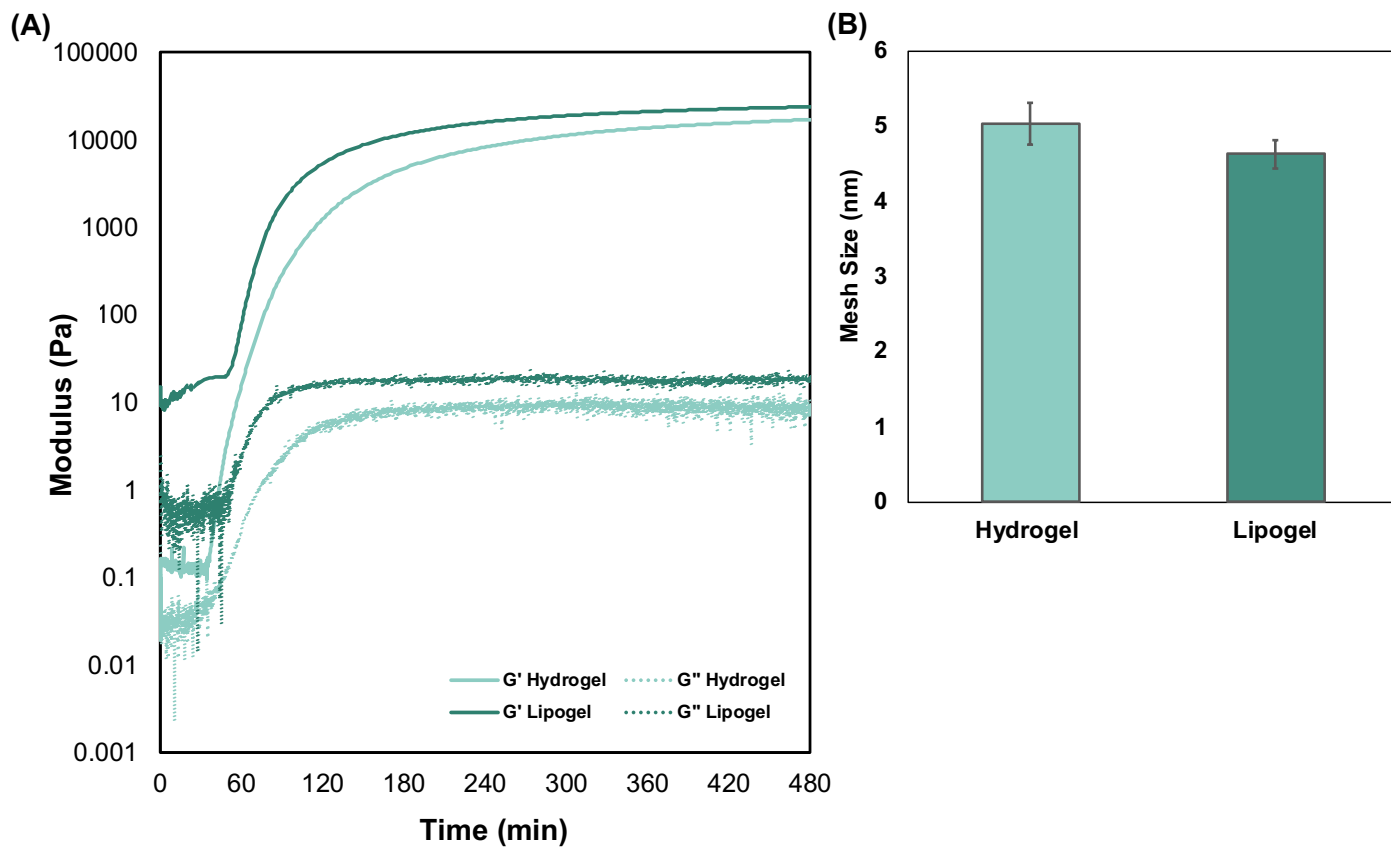


Figure S2: (A) In-situ bulk oscillatory rheology of 10wt% PEG-SH₄ (5kDa) PEG-VS₄ (5kDa) hydrogel (light teal) and 10wt% PEG-SH₄ (5kDa) PEG-VS₄ (5kDa) lipogel (dark teal) and (B) mesh size of hydrogel and lipogel, no significance.

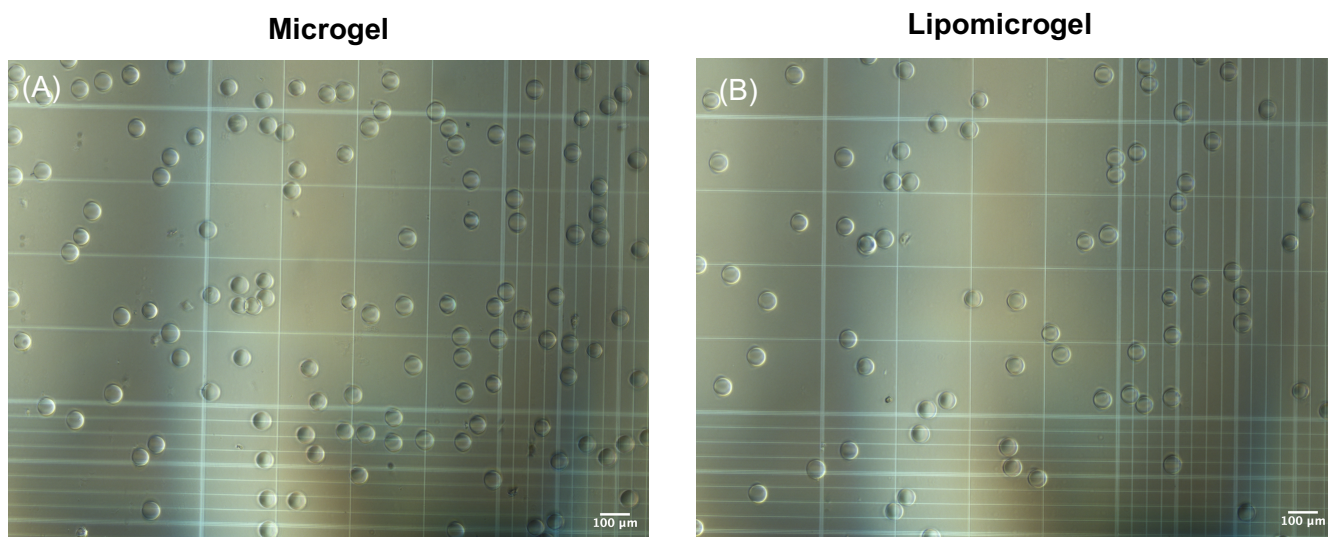


Figure S3: Bright field images of (A) microgels and (B) lipomicrogels on hemacytometer grid obtained on a Nikon Eclipse Ti microscope with a 10x objective.

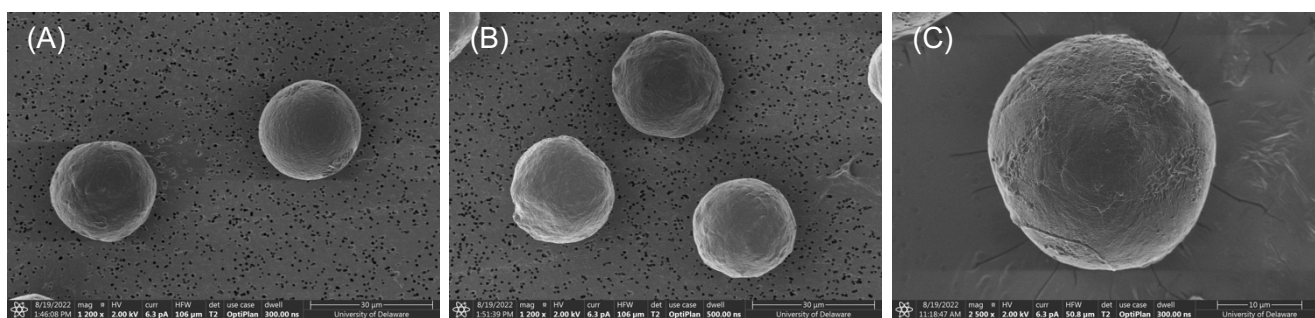


Figure S4: SEM images of microgels at 200 x magnification (A,B) and 500 x magnification (C). Microgels were placed onto SEM stubs containing a carbon tape substrate. Stubs were sputter coated with 5nm platinum in a Leica EM ACE600. A Thermo Scientific Apreo SEM was used to image the particles using a secondary electron detector at 2.0kV and 6.3pA.

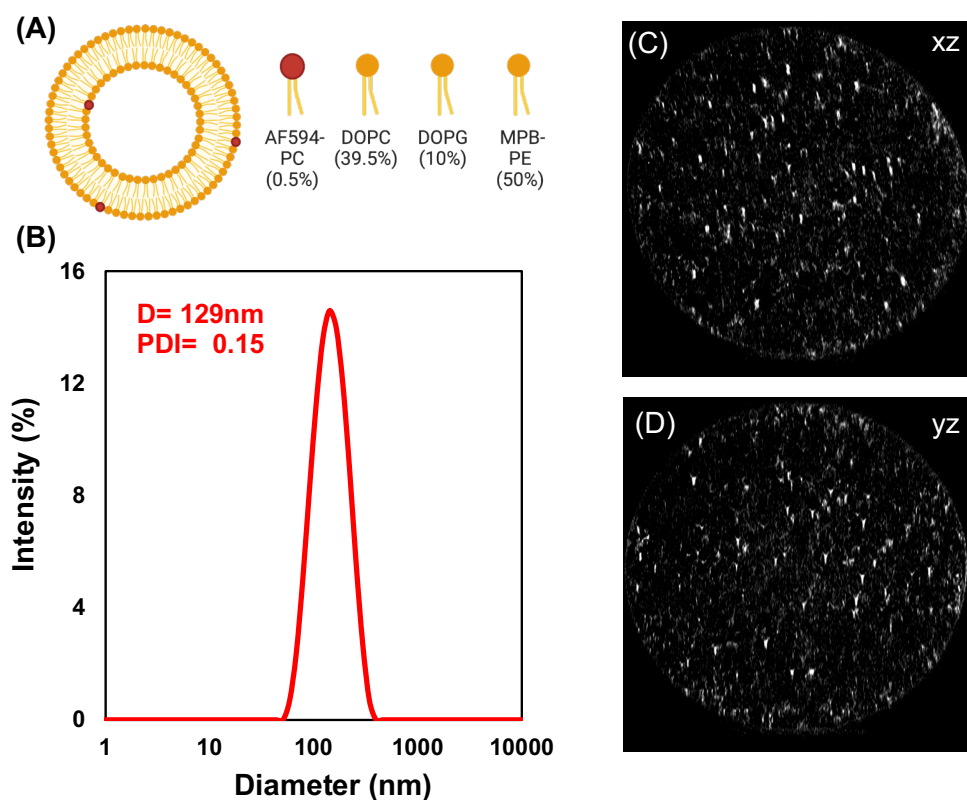


Figure S5: (A) Schematic representation and Liposomal formulation of fluorescently tagged liposomes used for imaging analysis. (B) Size distribution characterized by dynamic light scattering (C,D) xz and yz planes from lipo-microgel z-stack obtained via confocal microscopy.

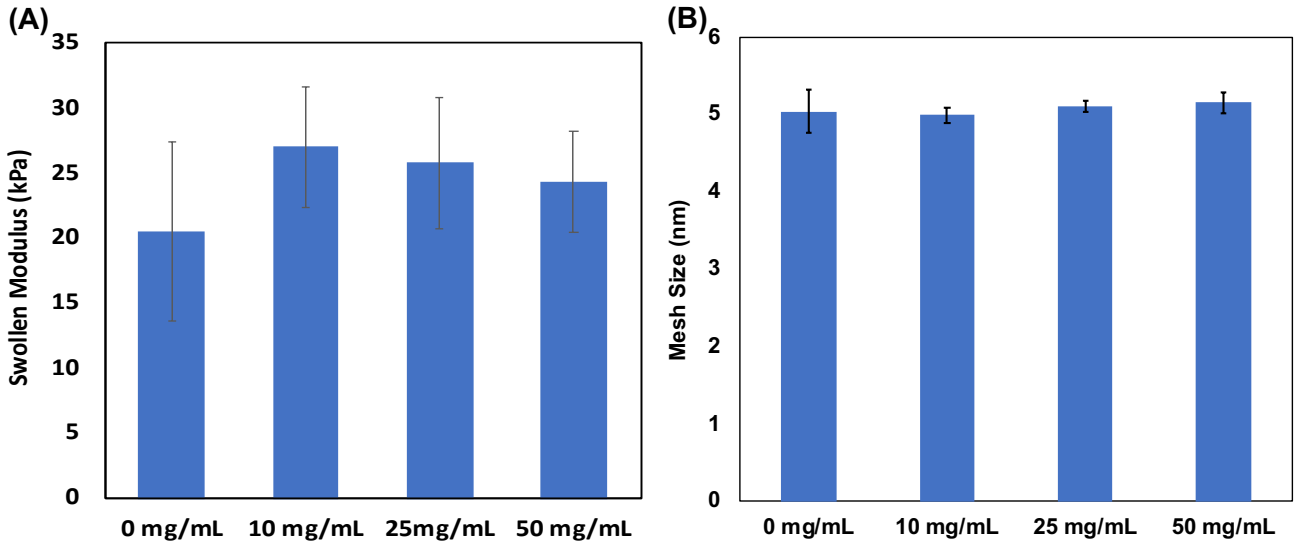


Figure S6: (A) Swollen modulus and mesh size of bulk hydrogels composed of 10 wt% (PEG-SH₄ + PEG-VS₄) with increasing concentrations of equine myoglobin (0, 10, 25, and 50 mg/mL), no significance. (B) Mesh size was calculated using the Flory-Rehner equation (shown as Equations 1-3) following protocols previously reported from our group^{1,2}, no significance.

Mesh Size Calculation

The mesh size was calculated using the Flory-Rehner equation, below adapted from past publications in our group^{1,2}.

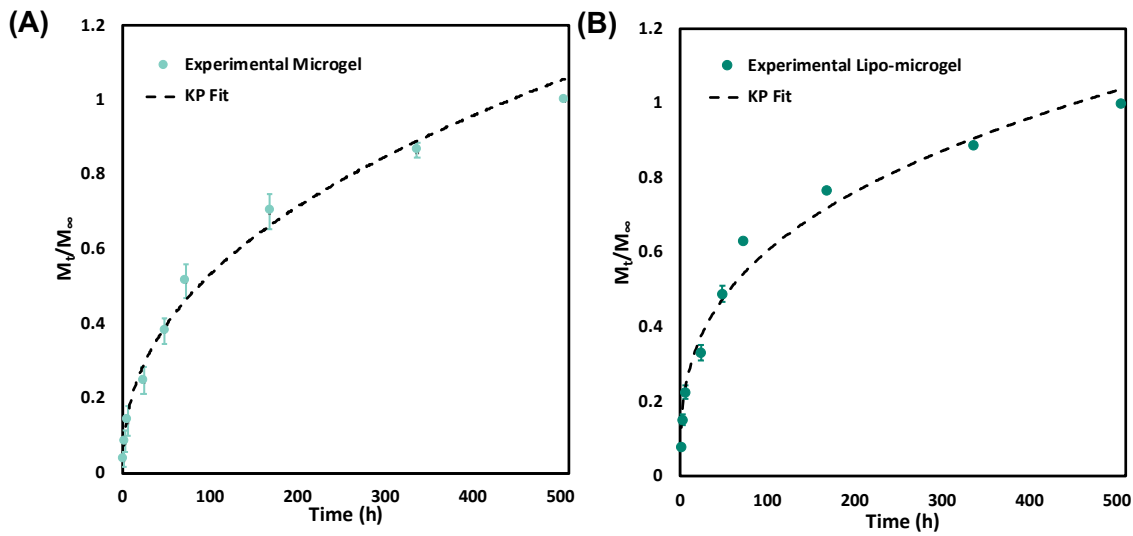
$$\frac{1}{\bar{M}_c} = \frac{2}{\bar{M}_n} - \frac{(\bar{v}/V_1)(\ln(1-v_2)+v_2+\chi_1 v_2^2)}{v_2^{1/3}-(v_2/2)} \dots \text{(Equation S1)}$$

\bar{M}_c is the average molecular weight between crosslinks, \bar{M}_n is the number average molecular weight of the uncrosslinked macromolecular chain (in our case 7,500 g/mol), \bar{v} is the specific volume of the polymer (0.833 cm³) is the molar volume of the solvent (for water, 18 cm³/mol), v_2 is the equilibrium volume fraction ($v_2 = Q - 1$), where Q was determined experimentally from swelling capacity (e.g. dry hydrogel volume divided by swollen hydrogel volume), and χ_1 is the polymer-solvent interaction parameter which is 0.44 for a PEG-water system. The unperturbed root-mean-square end-to-end distance ($(\bar{r}_0^2)^{1/2}$) was calculated via the following:

$$((\bar{r}_0^2)^{1/2}) = l C_n^{1/2} \left(\frac{2\bar{M}_c}{M_r}\right)^{1/2} \dots \text{(Equation S2)}$$

Where l is the average bond length (1.46 Å), C_n is the characteristic ratio PEG, in our case 4, and M_r is the molecular weight of the polymer repeat unit, which is 44 g/mol for PEG. Taken together the mesh size was calculated using the following³:

$$\xi = v_2^{-1/3} (\bar{r}_0^2)^{1/2} \dots \text{(Equation S3)}$$



(C)

	K_{kp}	n	R^2
Microgel	0.075 ± 0.021	0.42 ± 0.04	0.99
Lipo-microgel	0.131 ± 0.011	0.33 ± 0.01	0.98

Figure S7: Cumulative release curves for (A) microgels and (B) lipo-microgels where the filled circles represent experimentally collected data and the dashed lines are the corresponding mathematical fits via the Korsmeyer-Peppas equation. (C) Table for microgel and lipo-microgel constants for Korsmeyer-Peppas model fitting. Fractional release was calculated assuming equilibrium conditions at the end of the 3 week experiment.

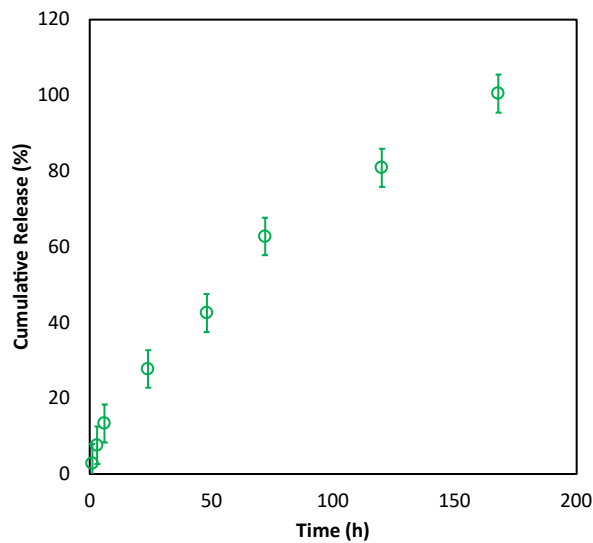


Figure S8: Cumulative release of 4K-FITC-Dextran from liposomes alone.

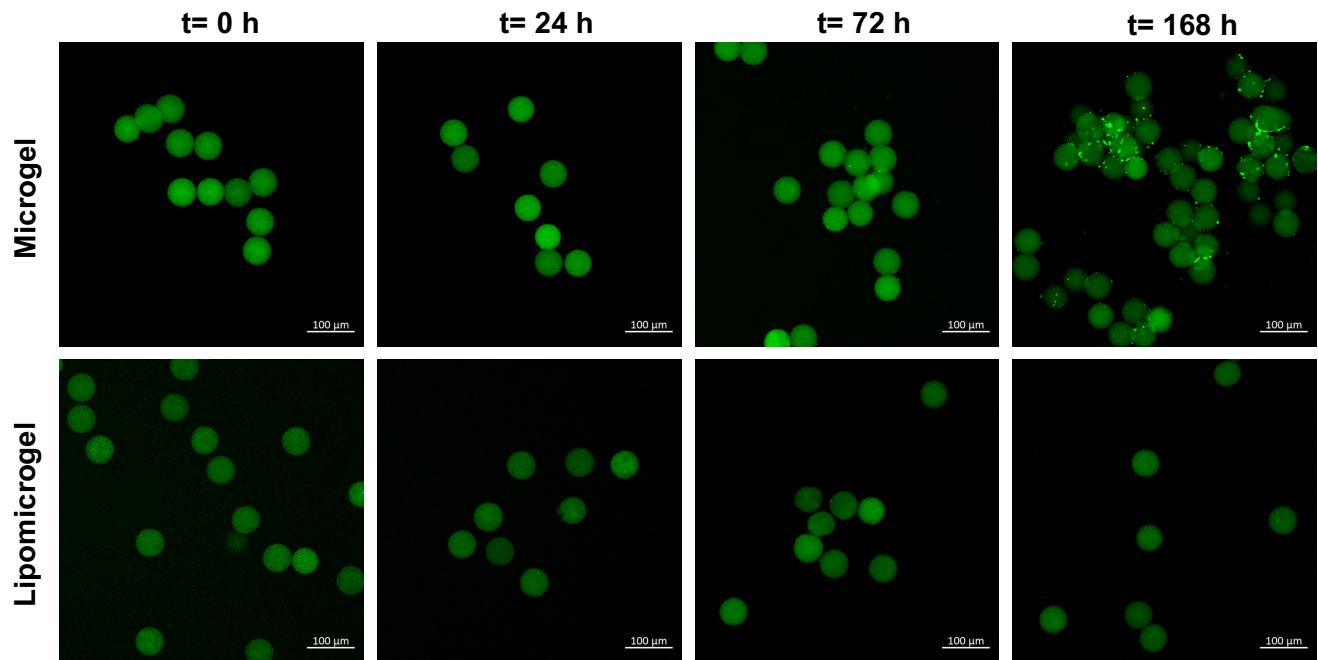


Figure S9: Confocal microscopy of FITC-Dextran loaded microgels and lipomicrogels over 1 week timeframe.

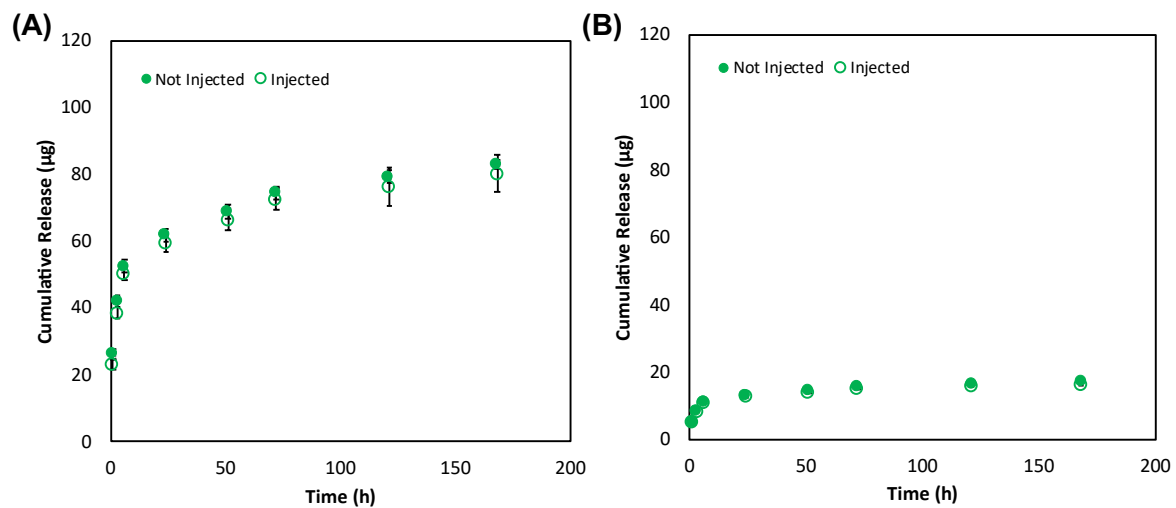


Figure S10: Release of FITC-DEX over one week from microgels (A) and lipo-microgels (B) either not injected or injected through a 27.5 G needle. Error bars represent standard deviation and are not visible in (B) due to marker size and scale. The release experiments performed for this study were done differently than those that appear in the main text. Rather than use a dialysis cup, the

microgels suspensions were centrifuged at 1,200 rcf for 10 minutes and an aliquot of the supernatant was collected at each timepoint (1,3,6,24,48,72,120, and 168 hrs). Measurement of the release samples and generation of the cumulative release curves follows analyses performed in the main text.

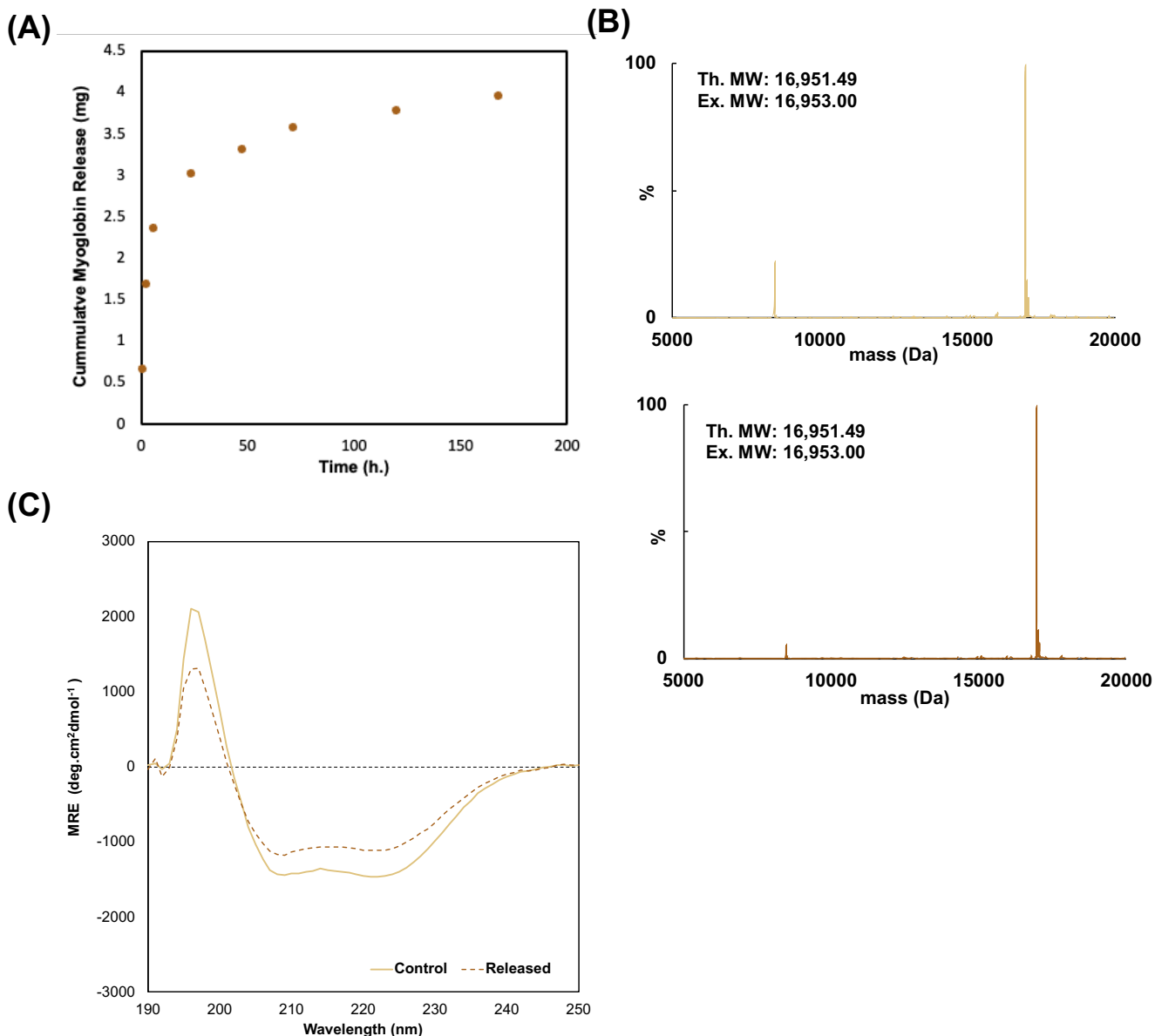


Figure S11. Protein stability following release (A) Cumulative release of myoglobin from microgels **(B)** Electrospray ionization mass spectrometry of myoglobin before (top) and after (bottom) release from microgels. Theoretical MW 16,951.49 Da Experimental MW 16,953. **(C)** Circular dichroism of equine myoglobin before and after release from microgels 70 μ M in 0.1X PBS at room temperature. CD experiments were performed at room temperature using a Jasco J-1500 CD spectropolarimeter (Jasco, Easton MD) with a 0.1 cm path length quartz cuvette containing 100 μ L of sample.

References:

1. P.J. Flory, Principles of Polymer Chemistry: Cornell University Press, **1953**.
2. R.A. Scott et.al., *Adv. Healthcare Mat.*, **2020**.
3. T. Canal, et.al., *J. Biomed. Mater. Res.*, **1989**.